Bayesian analysis for estimating statistical parameter distributions of elasto–viscoplastic material models

Aritra Chakraborty*, M. C. Messner

Applied Materials Division, Argonne National Laboratory

Abstract

High temperature design methods rely on constitutive models for inelastic deformation and failure typically calibrated against the mean of experimental data without considering the associated scatter. Variability may arise from the experimental data acquisition process, from heat-to-heat material property variations, or both and need to be accurately captured to predict parameter bounds leading to efficient component design. Applying the Bayesian Markov Chain Monte Carlo (MCMC) method to produce statistical models capturing the underlying uncertainty in the experimental data is an area of ongoing research interest. This work varies aspects of the Bayesian MCMC method and explores their effect on the posterior parameter distributions for a uniaxial elasto–viscoplastic damage model using synthetically generated reference data. From our analysis with the uniaxial inelastic model we determine that an informed prior distribution including different types of test conditions results in more accurate posterior parameter distributions. The parameter posterior distributions, however, do not improve when increasing the number of similar experimental data. Additionally, changing the amount of scatter in the data affects the quality of the posterior distributions, especially for the less sensitive model parameters. We also test some of these inferences against real experimental tensile and creep data of Grade 91 steel at 600 °C and observe consistent results. Moreover, we perform a sensitivity study of the model parameters against the likelihood function prior to the Bayesian analysis. The results of the sensitivity analysis help to determine the reliability of the posterior distributions and reduce the dimensionality of the problem by fixing the insensitive parameters. The comprehensive study described in this work demonstrates how to efficiently apply the Bayesian MCMC methodology to capture parameter uncertainties in high temperature inelastic material models. Quantifying these uncertainties in inelastic models will improve high temperature engineering design practices and lead to safer, more effective component designs.

Keywords: Statistical modeling, inelastic parameters, high temperature, sensitivity analysis, Markov Chain Monte Carlo

1. Introduction

A better understanding of uncertainty of structural degradation in high temperature components could lead to safer, more efficient component designs. Despite successes in other indus-

*Corresponding author. Tel: +1 630 252-6523
Email address: achakraborty@anl.gov (Aritra Chakraborty)

tries, probabilistic design through risk-informed or reliability-based design and inspection has not been widely applied to high temperature structural components. With the exception of a few general applications (c.f. [1–3]) most existing probabilistic analyses for high temperature components focus on creep crack growth [4, 5]. Several factors limit the application of probabilistic design to high temperature components — limited material test data, a poor understanding of uncertainty in component loading conditions, and difficulty in analyzing individual components separate from plant systems. However, inelasticity poses perhaps the most substantial obstacle.

Many practical design methods for low temperature applications avoid requiring a full probabilistic structural analysis by assuming a linear elastic response while accounting for uncertainty in the loads and in the material strength (c.f. [6]). This approach is unsuitable at high temperatures where material inelasticity, via creep, occurs even below the yield point in the classical elastic regime. This paper describes a first attempt at quantifying uncertainty in inelastic models of high temperature deformation. A practical method accounting for this uncertainty is a key ingredient in applying probabilistic design concepts to high temperature structures.

The classical approach for identifying the parameters of a high temperature inelastic constitutive models is by minimizing the error between the model prediction and the equivalent experimental data, known as the inverse analysis [7]. Most of the existing literature focuses on estimating these model parameters deterministically [8–19]. Studies range from simple isotropic one-dimensional models to anisotropic microstructure-informed crystal plasticity models, coupled to several types of optimization algorithms. A critical shortcoming of this deterministic approach is it neglects the scatter associated with the experimental data due to measurement or material variability, which can only be captured through statistical modeling [20]. Probabilistic parameter estimation for viscoplastic material models is an active research area and limited studies exist in the literature. Harth et al. [21] performed statistical Monte Carlo simulations to generate artificial data that mimicked the observed experimental scatter in order to obtain a distribution of the model parameters, along with mean, standard deviation, and coefficient of variation values. Bayesian analysis is a suitable approach to incorporate uncertainties in the material response for estimating parameter distributions that successfully captures the observed scatter in the experiments [22].

The key output of Bayesian analysis are the probability distributions of the properties of interest, called the posterior distributions. This approach incorporates existing knowledge about the system of interest through the prior distributions of the parameters which then update depending on the likelihood function to improve the corresponding posterior distributions following the Bayes' rule. Sampling strategies are a crucial component of Bayesian inference with most studies selecting the Markov Chain Monte Carlo (MCMC) sampling approach. Rappel et al. [23] used Bayesian analysis with the Markov Chain Monte Carlo (MCMC) sampling algorithm to identify the Young's modulus for a linear elastoplastic material model taking into account experimental scatter and noise. Fitzenz et al. [24] used the hierarchical Bayesian approach to identify the distribution of parameters for non linear creep models. Madireddy et al. [25] applied Bayesian analysis for hyperelastic material models describing soft tissues to better represent the scatter in the experimental data.

The Bayesian approach required depends strongly on the system being investigated. For example, Madireddy et al. [25] reported a limited influence of the prior distribution on the posterior for hyperelastic material models, while Rappel et al. [26] observed a significant effect of the prior for viscoelastic material models. Gang et al. [27, 28] and Asaadi and Heyns [29] used Bayesian MCMC to obtain posterior parameter distributions for three dimensional viscoplastic model parameters and mimicked the three dimensional finite element response, required for calculating

the likelihood, with surrogate models. Yeratapally et al. [30] performed uncertainty quantification for microstructure-based viscoplastic parameters by performing full-field crystal plasticity simulations. Janouchová and Kučerová [31] calibrated the isotropic and kinematic hardening parameters of a one-dimensional material model for copper alloys using repeated uniaxial cyclic test data.

Even though the aforementioned studies use Bayesian approach, they do not assess the stability of the resulting posterior distributions against different aspects of the method, such as choice of prior distributions, amount of data, amount of scatter in the experimental data, as well as the accuracy of the final posterior distributions. In this work, we examine these aspects of the Bayesian MCMC approach for a one dimensional elasto–viscoplastic material model parameters using both synthetically generated experimental data and real experimental data for monotonic tension and creep experiments. With synthetic reference data we can accurately quantify the reliability and accuracy of the posterior distributions, given the a priori knowledge of the true solution [32]. Determining the capabilities and shortcomings of the Bayesian approach is crucial in effectively using the method for engineering design.

The paper is structured as follows: Section 2 describes the one dimensional elasto–viscoplastic damage model used in this work, provides a brief review of the Bayesian approach, and describes the generation of the artificial experimental data. Section 3 highlights the important results of the study for both synthetic and real experimental data and Section 4 discusses the critical inferences from the analysis. Finally, Section 5 summarizes the key findings of this work.

2. Simulation details

2.1. Elasto–viscoplastic damage model:

The one-dimensional material model used in this study is based on small strain deformation theory where the total strain rate is the sum of the elastic and viscoplastic strain rate components:

$$\dot{\epsilon} = \dot{\epsilon}_e + \dot{\epsilon}_{vp} \tag{1}$$

with the elastic strain rate following Hooke's law

$$\dot{\epsilon}_e = E\dot{\sigma} \tag{2}$$

where E is the Young's modulus. The inelastic strain rate follows the Perzyna flow rule [33] with damage,

$$\dot{\epsilon_{vp}} = \left\langle \frac{\frac{\sigma}{1-\omega} - \sigma_0 - R}{\eta} \right\rangle^n, \tag{3}$$

where ω is the damage variable, and n, η and σ_0 are the viscoplastic parameters. The hardening internal variable R follows a standard isotropic Voce hardening law, [34],

$$R = Q\left[1 - \exp\left(-b\left|\epsilon_{vp}(t)\right|\right)\right] \tag{4}$$

where b and Q are the hardening parameters. The damage rate is the classical model by Leckie and Hayhurst [35],

$$\dot{\omega} = \left(\frac{\sigma}{A}\right)^{\zeta} (1-\omega)^{-\phi} \tag{5}$$

where A, ϕ and ζ represents the adjustable damage parameters. The elasto–viscoplastic damage model described above is suitable only for monotonic loading, which is the focus of the present work. The concepts discussed here could be applied to cyclic plasticity models with kinematic hardening terms, albeit at greater computational cost. Given that design approaches often assume a monotonic, steady-state response (for example primary load design in the ASME Boiler & Pressure Vessel Code), the monotonic models discussed here are relevant to engineering practice and form a useful starting point for more complicated descriptions of inelasticity.

We solve these coupled equations for one-dimensional tensile and creep boundary conditions to obtain the simulated material response. Additionally, to reduce computation time for the creep tests that involve large time scale simulations, we use the following semi-explicit method to calculate creep strain at different times for constant stress conditions:

1. Calculate the current damage $\omega(t)$ from the analytical damage equation, the integral of Eq. (5) under constant stress condition,

$$\omega(t) = 1 - \left(1 - \frac{t}{\left(\frac{\sigma}{A}\right)^{-\zeta}(1+\phi)^{-1}}\right)^{\frac{1}{1+\phi}} \tag{6}$$

2. Assume an explicit dependence of hardening $\dot{R}$ on strain rate, i.e., the current hardening of the material $R(t)$ depends on the known creep (viscoplastic) strain from the previous time step, $\epsilon_{vp}(t - dt)$,

$$R(t) = Q\left[1 - \exp\left(-b\left|\epsilon_{vp}(t - dt)\right|\right)\right] \tag{7}$$

3. Finally solve for the current creep strain, $\epsilon_{vp}(t)$, by numerically integrating Eq. (3) using the damage and hardening values obtained from Eq. (6) and Eq. (7) respectively,

$$\epsilon_{vp}(t) = \epsilon_{vp}(t - dt) + dt\left\langle\frac{\frac{\sigma}{1-\omega(t)} - \sigma_0 - R(t)}{\eta}\right\rangle^n \tag{8}$$

This explicit integration is accurate for long-term creep tests where the model internal variables change slowly with time. We compared the results from this semi-explicit scheme to a fully-implicit time integration and the differences between the two approaches were negligible for the creep conditions considered here. For the tensile tests, we solve the full implicit system of equations, as these simulations are relatively inexpensive due to the low total tensile deformation (a total strain of 3 %).

For a reasonable assumption of the prior distributions for performing the Bayesian Markov Chain Monte Carlo (MCMC) analysis we first calibrate the elasto–viscoplastic damage model. The model has 5 inelastic deformation parameters $(n, \eta, \sigma_0, Q, b)$, and 3 damage parameters (A, ζ, ϕ). In this work the Bayesian MCMC analysis with synthetic experimental data assumes the inelastic parameters to lie within bounds specified in Table 1 and fixes the damage parameters to values as listed in Table 1. The bounds of the inelastic parameters are based on their calibrated values for Grade 91 steel at 550 °C, and reasonably bound the actual material behavior [36]. Fixing the damage parameters is reasonable as their mean and distribution can be obtained

Table 1: Bounds for the inelastic parameters of the model.

parameter	Bounds
n	$[9, 13]$
η	$[700, 950]$
σ_0	$[2, 10]$
Q	$[80, 130]$
b	$[40, 70]$
A	517.0
ζ	12.5
ϕ	2.5

from Larson–Miller fits to rupture data, and the focus in this work is primarily on material deformation. [1]

Uncertainties in measured experimental data can be broadly classified into either aleatory or epistemic uncertainties [37–39]. Aleatory uncertainties are the inherent uncertainties associated with the physical system or environment, while epistemic uncertainties arise from imperfect knowledge of the system or the inaccuracy of the model, and presumably reduces with sufficient data. This study analyzes the epistemic uncertainties in the material response using Bayesian Markov Chain Monte-Carlo (MCMC) analysis.

In Bayesian analysis the probability of the model parameters, $\boldsymbol{\alpha}$, given the data, D, the posterior distribution, $\boldsymbol{\pi}(\boldsymbol{\alpha}|D)$, updates according to the Bayes' theorem:

$$\boldsymbol{\pi}(\boldsymbol{\alpha}|D) = \frac{\boldsymbol{\pi}(D|\boldsymbol{\alpha})\,\boldsymbol{\pi_0}(\boldsymbol{\alpha})}{\boldsymbol{\pi}(D)} \tag{9}$$

where $\boldsymbol{\pi_0}(\boldsymbol{\alpha})$, represents the initial prior distribution constructed from prior knowledge about the system [40]. The likelihood, $\boldsymbol{\pi}(D|\boldsymbol{\alpha})$, on the other hand represents the likelihood of observing the data, D, given the parameter realizations, $\boldsymbol{\alpha}$. Most studies treat the denominator, $\boldsymbol{\pi}(D)$, which represents the probability of the data, as a normalization factor, thus allowing the following simplified relationship between the posterior, prior, and the likelihood distributions:

$$\boldsymbol{\pi}(\boldsymbol{\alpha}|D) \propto \boldsymbol{\pi}(D|\boldsymbol{\alpha})\,\boldsymbol{\pi_0}(\boldsymbol{\alpha}) \tag{10}$$

The analysis assumes $\boldsymbol{\pi}(D|\boldsymbol{\alpha})$ similar to [30], and its logarithm, $\mathcal{L}$, represents the likelihood function determining the acceptance or rejection of the sampled parameters,

$$\boldsymbol{\pi}(D|\boldsymbol{\alpha}) = \frac{1}{(2\pi\xi^2)^{\frac{n}{2}}} \exp \sum_{i=1}^{n} \left(\frac{-(y_i - g_i(\boldsymbol{\alpha}))^2}{2\xi^2} \right), \text{or,} \tag{11}$$

$$\mathcal{L} = \log\left(\boldsymbol{\pi}(D|\boldsymbol{\alpha})\right) \equiv \sum_{i=1}^{n} \left(\frac{-(y_i - g_i(\boldsymbol{\alpha}))^2}{2\xi^2} \right) \tag{12}$$

[1] Using the Larson–Miller parameter for Grade 91 steel and log-linear fit with the experimental rupture data the time to failure can be obtained as a function of stress at a given temperature. A similar relation can also be obtained by integrating the damage rate equation, i.e., by replacing $\omega = 1$ in Eq. (6). Comparing the two expressions gives the damage parameters satisfying the Larson–Miller relation.

where ξ is the hyper parameter representing the scatter in the available data. i represents the different test conditions for the tensile and creep experiments. y_i represents (synthetic or real) experimental tensile and creep results at the different test conditions, and $g_i(\boldsymbol{\alpha})$ represents the corresponding simulated results with the sampled parameter values $\boldsymbol{\alpha}$. The total likelihood is the weighted sum of individual likelihood values from tensile and creep data such that they contribute equally to the total likelihood. Thus, with unit standard deviation the likelihood function represents the square error between the experimental and the simulated results. We also scale the parameters between 0.0 and 1.0 for better sampling during the Bayesian MCMC analysis. This study implements the Bayesian analysis using the open-source python package PyMC3, [41], with the Metropolis–Hastings algorithm, [42], for the Monte-Carlo sampling [43], and runs five Markov chains in parallel to ensure convergence, with 500 draws and 300 discarded ('burn-in') points for each Markov chain.

2.2. Sensitivity analysis

This study assumes that the posterior distribution from the Bayesian analysis for each of the parameters depends strongly on their sensitivity to the likelihood function. To test this, we perform sensitivity analysis for each of the five inelastic parameters against the combined likelihood function (weighted sum of individual likelihood from tensile and creep boundary conditions) within the bounds specified in Table 1 with two different sensitivity analysis methods– Sobol's method [44] with the sampling scheme by Saltelli [45], and the Fourier Amplitude Sensitivity Test (FAST) method by Schaibly and Shuler [7], both available in the open source Sensitivity Analysis Library (SALiB) [46] package in Python. Similar to the Bayesian analysis, the parameters are scaled linearly between 0 and 1 for the sensitivity analysis.

2.3. Synthetic experiments

The synthetic data are tensile and creep simulations with the viscoplastic model for parameters drawn from normal distributions for each of the five inelastic parameters. The assumed uncoupled normal distributions have mean 0.5 and standard deviation 0.1 for all the parameters, scaled so that parameter values are in [0,1]. Figure 1 plots the variability for the tensile and the creep boundary conditions after sampling 20 parameter values from the distribution for a fixed strain rate and creep stress. Figure 2 shows synthetic experimental data for the tensile and creep tests with 30 different test conditions used in this work. The different test conditions (different colored curves in Fig. 2) include strain rates spanning linearly between 1×10^{-5} and 1×10^{-3} s^{-1} for tensile tests, and stresses between 100 and 200 MPa for creep tests. The choice of these values reflect reasonable experimental conditions for high temperature materials.

3. Results

3.1. Sensitivity analysis

Table 2 lists the sensitivity values of the inelastic parameters within the bounds as listed in Table 1, applying two different sensitivity analysis methods. The objective function for the sensitivity analysis is the combined likelihood function from tensile and creep synthetic experiments at 10 different test conditions (10 different curves from each (a) and (b) in Fig. 2) with a unit standard deviation, ξ, in the likelihood function. The likelihood function with unit standard deviation resembles sum of square errors often used as the objective function for minimization in deterministic calibration. The results from both sensitivity analysis methods are similar, with n

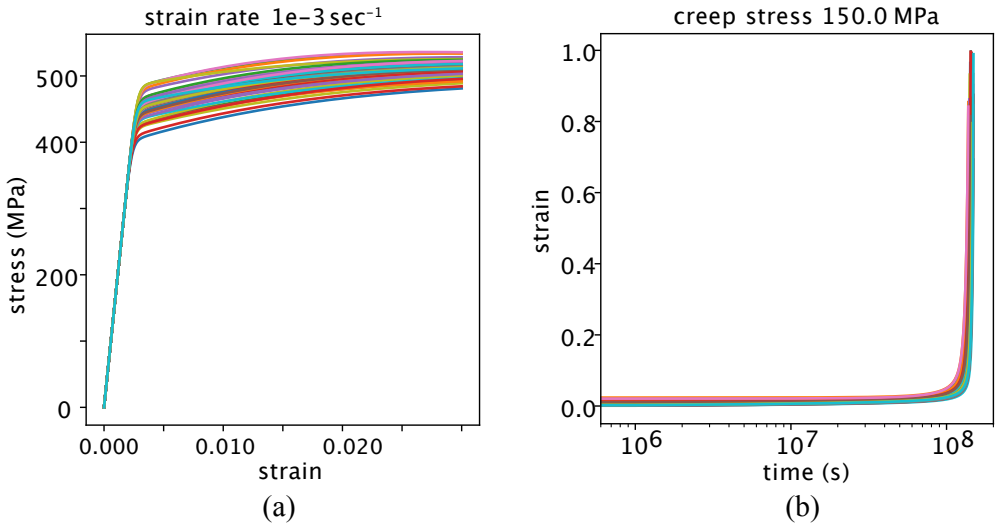

Figure 1: Variability in the tensile (a) and creep (b) response at a fixed strain rate and creep stress respectively, with 20 draws of parameter values with the target distribution of a truncated normal.

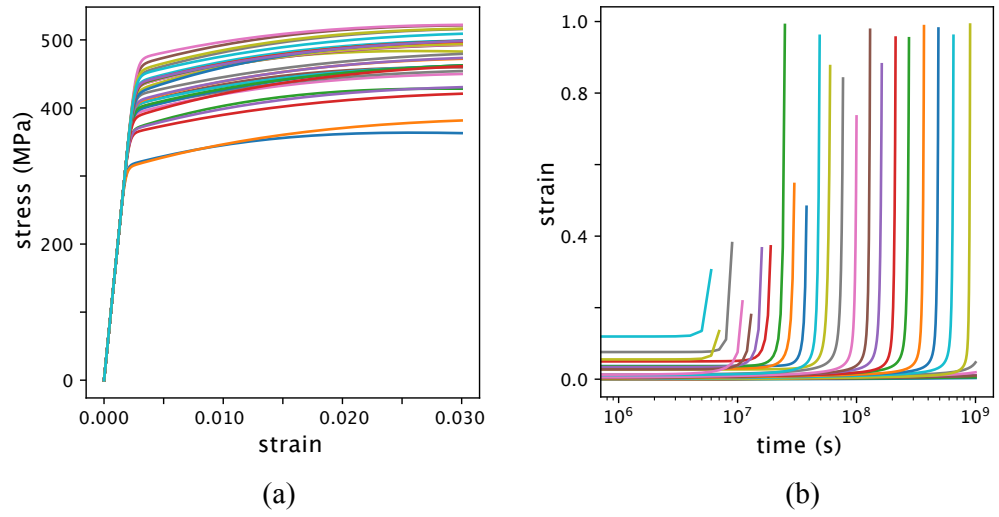

Figure 2: Synthetic experimental data for 30 different tensile, (a), and creep, (b), tests. Different colors correspond to different test conditions, i. e., strain rates for tensile tests and stresses for creep tests.

Table 2: Sensitivity values of the inelastic parameters.

parameter	Sobol	FAST
n	0.797247	0.771342
η	0.792725	0.815553
σ_0	0.007422	0.006315
Q	0.066374	0.049494
b	0.059265	0.054965

and η being the most sensitive parameters followed by the hardening parameters Q and b, and σ_0 being the least sensitive parameter. The sensitivity values are qualitative as their relative difference does not necessarily represent their quantified influence on the likelihood function.

Subsequently, using synthetic experimental data we compare the effects of the different aspects of the Bayesian MCMC framework such as the prior distribution, quantity of reference data, including different type of experiments, and reference data scatter on the accuracy of the posterior distribution. We then test some of these aspects with real experimental data. Figures 3 to 6, 8 and 9 compare the posterior distributions (blue histograms and the red curves) of the five inelastic parameters to their respective priors (black dashed curves) and target distributions (green dashed curves) for synthetic reference data. Comparing the posterior means and standard deviations (shown within brackets in top corner in each plot) to their true values, and the respective Kolmogorov-Smirnov (KS) values quantifies the differences between the target and the posterior distributions. The KS values determine the similarity between the posterior distributions and their corresponding target, with lower values representing more similar distributions.

Effect of prior distribution. For the Bayesian MCMC analysis the prior distribution generally requires some information about the problem. Most studies on Bayesian analysis prefer a uniform prior distribution as it requires limited information about the model parameters. However, here a uniform (uninformed) prior distribution may lead to prematurely converged result from the Bayesian MCMC analysis. To investigate this, we compare the posterior distributions when selecting a uniform prior distribution to that of a truncated normal prior distribution for each of the five inelastic parameters within the assumed bounds. The truncated normal prior distributions assume mean and standard deviation of 0.3 and 0.2 for all the five inelastic parameters (black dashed lines in Fig. 3), while their target distributions (used to generate the reference data) are also truncated normal distributions with mean and standard deviation of 0.5 and 0.1, respectively (green dashed lines in Fig. 3). The synthetic experimental reference for the Bayesian analysis consists of 10 different datasets for the tensile and creep conditions (representing 10 different strain rates and creep stresses) while the standard deviation, ξ, in the likelihood function is fixed to unity for both tensile and creep cases. Figure 3 compares the two posterior distributions obtained from a uniform prior distribution and a truncated normal prior distribution for each of the five inelastic parameters. KS values with a truncated normal prior are lower than that for the uniform prior distribution, while the prior distribution remains almost unchanged for the least sensitive parameter σ_0. The distribution type is recovered for the most sensitive parameters (n and η) for both cases, however, with the uniform prior distribution the resulting posterior means are far away from the target.

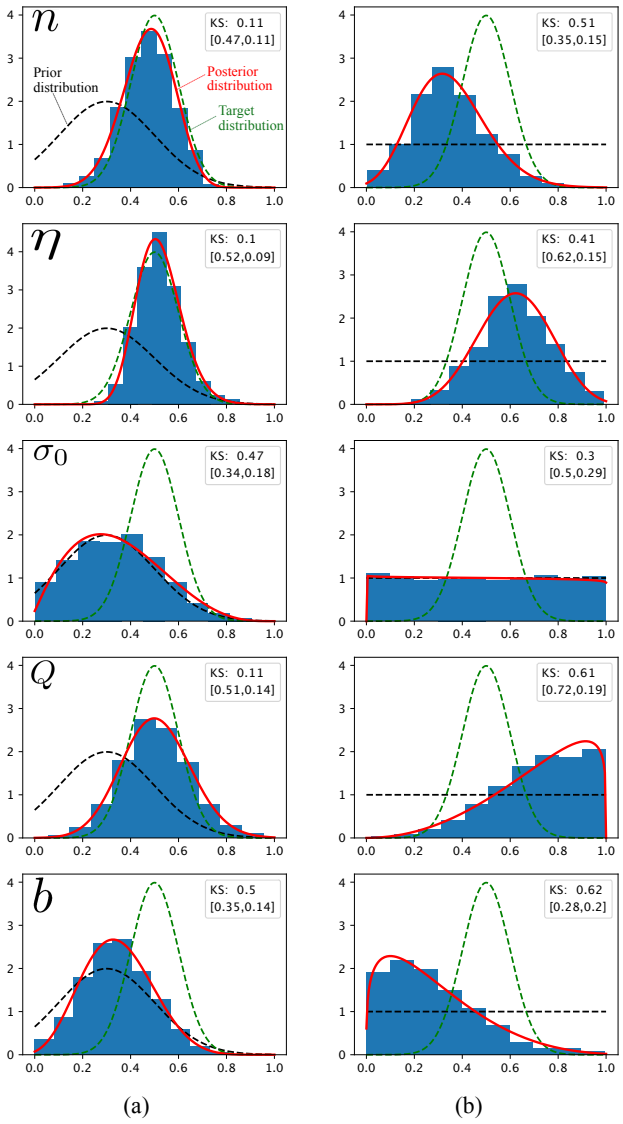

Figure 3: Posterior distributions from a truncated normal prior with mean 0.3 and standard deviation of 0.2, (a), and a uniform prior, (b), for the five inelastic parameters, fitted to a β-distribution, red curves. The figure shows the normalized histogram for each of the parameters (in blue) such that the integral of their probability density adds up to one. The black and the green dashed curves represent the assumed prior and the resulting posterior distributions of the parameters, respectively. The values in the corner shows the mean (left) and standard deviation (right) of the values obtained from the Bayesian MCMC analysis (for example in top figure in (a), i. e. for parameter n, [0.47, 0.1] correspond to a mean of 0.47 and standard deviation of 0.1). The corresponding target mean and standard deviation are 0.5 and 0.1, respectively, for all parameters. As a comparison between the posterior (histogram data) and the target (green dashed curve), the goodness of the fit described by the Kolmogorov-Smirnov (KS) value also appears in the top corner for each of the parameter. All subsequent plots with synthetic reference data follow this layout.

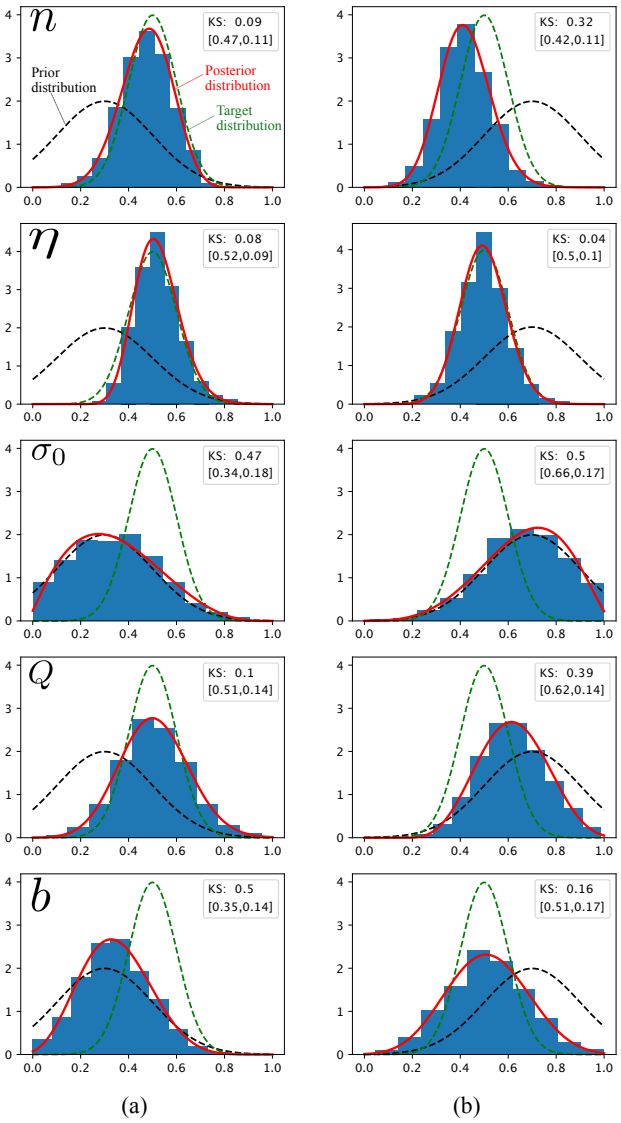

Figure 4: Posterior distributions from truncated normal priors with mean 0.3, (a), and 0.7, (b), and standard deviations of 0.2 (for both), for the inelastic five parameters.

Effect of prior means. From the previous analysis we find that an informed prior (truncated normal distribution) better recovers the true solution when compared to an uninformed prior. Using the same synthetic reference data (10 tensile and 10 creep curves) and likelihood function ($\xi = 1$) we compare the stability of the posterior distributions for two different truncated normal distribution priors, i.e., having different means of 0.3 and 0.7, but with same standard deviation of 0.2. For both posterior distributions in Fig. 4, the means for the two most sensitive parameter,

n and η, are very close to the true solution. For the hardening parameters, Q and b, the posterior distribution resembles the expected distribution (i.e., a truncated normal distribution), however, the analysis fails to accurately recover the true mean values of b and Q when starting with prior means of 0.3 and 0.7 respectively. The posterior distribution for the least sensitive parameter σ_0 is the least accurate and hardly changes from the prior.

Effect of increasing the available data. To investigate whether adding more tensile and creep reference data affects the Bayesian MCMC process we compare the posterior distributions obtained with 5 and 30 datasets for each tensile and creep experiments (sampled from Fig. 2) for the likelihood ($\xi = 1$). Both cases start with the same prior distribution (truncated normal with mean 0.3 and standard deviation 0.2) for the five inelastic parameters, and Fig. 5 shows the posterior distributions. The amount of data has limited influence on the posterior distributions of the parameters with synthetically generated experimental data. This implies that a small amount of data correctly capturing the underlying parameter distributions is sufficient to predict the accurate posterior distributions. Moreover, increasing the amount of data does not influence the sensitivity of the parameters to the likelihood.

Effect of dimensional reduction. We also check whether a dimensional reduction of the parameter space by fixing the least sensitive parameter, σ_0, increases the efficiency of the Bayesian MCMC algorithm to better estimate the posterior distributions of the hardening parameters Q and b. Figure 6 shows the posterior distributions for the four inelastic parameters starting from a truncated normal prior distribution having a mean of 0.3 and a standard deviation of 0.2 for all parameters (dashed black curves in Fig. 6). The reference data consists of 10 tensile and 10 creep tests and a unit standard deviation in the likelihood function. Fixing σ_0 hardly affects the posterior distributions of hardening parameters, suggesting lack of correlation between σ_0 and the other parameters.

Effect of including different type of tests. The previous Bayesian MCMC analysis with the tension and creep tests as reference accurately recovers only the most sensitive inelastic parameters n and η. In order to improve the the posterior distributions of the lesser sensitive hardening parameters (Q and b) we repeat the Bayesian MCMC analysis with five additional strain rate jump tension tests shown in Fig. 7. Figure 8 compares the posterior distributions of the five inelastic parameters from the Bayesian MCMC including the jump tests with 10 tensile and creep tests ((b) and (d)) to the posteriors only considering the tension and creep tests ((a) and (c)). The results also compare the posteriors from two different truncated prior normal distributions with mean 0.3 and standard deviation of 0.2 ((a) and (b)), and with mean of 0.7 and standard deviation of 0.2 ((c) and (d)). The posterior distributions (red solid curves) of the lesser sensitive hardening parameters (Q and b) for both prior distributions are closer to their corresponding expected distributions (green dashed lines), while the posterior of the least sensitive parameter, σ_0, hardly changes.

Effect of scatter in the experimental data. For all of the above analysis the standard deviation, ξ, in the likelihood function,

$$\mathcal{L} = \sum_{i=1}^{n} \left(\frac{-(y_i - g_i(\boldsymbol{\alpha}))^2}{2\xi^2} \right), \tag{13}$$

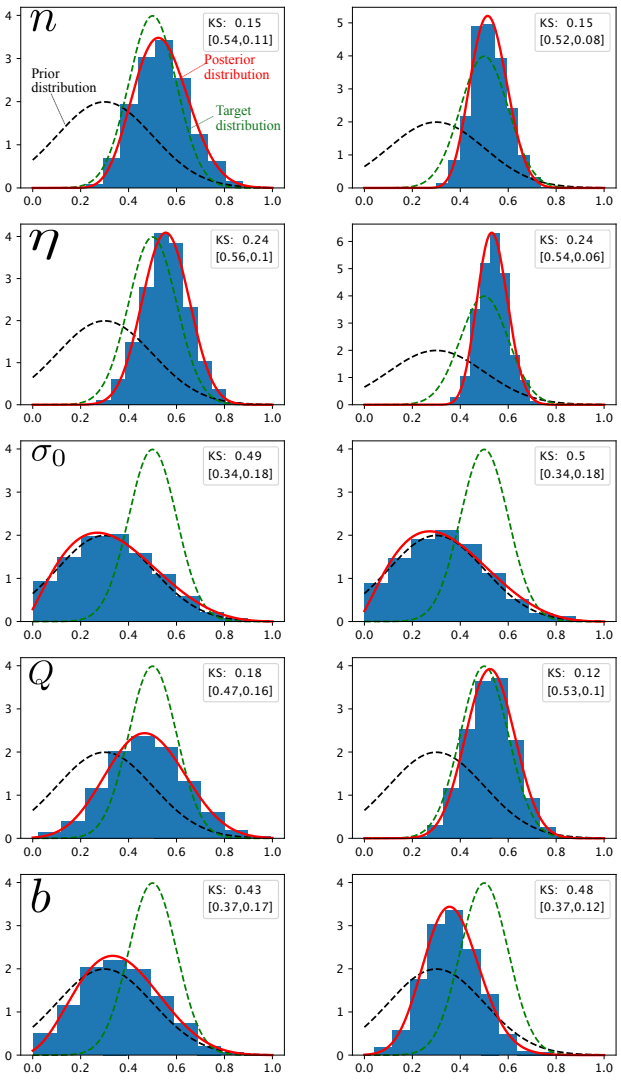

Figure 5: Posterior distributions with truncated normal prior distribution with mean 0.3 and standard deviation of 0.2 for all five parameters obtained with 5, (a), and 30, (b), datasets for each of the tensile and creep conditions. For the synthetic datasets increasing the amount of reference data seems to hardly influence the posterior distributions.

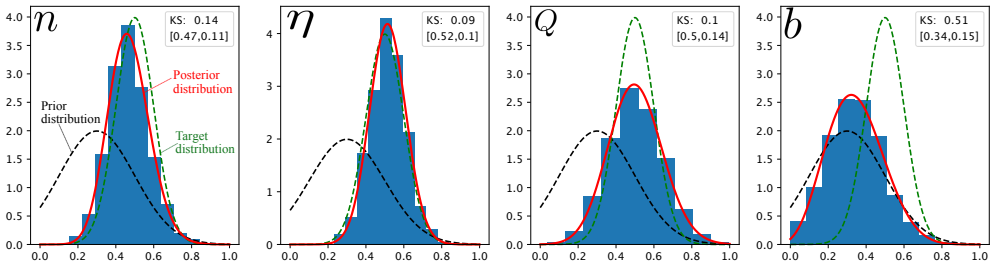

Figure 6: Posterior distributions from truncated normal priors with mean 0.3 and standard deviation of 0.2 for the four most sensitive parameters (black dashed curves). Fitted β-distributions are shown in red curves with the normalized histogram of the posterior values in blue. Dimensional reduction does not improve the posterior distribution of the hardening parameter b.

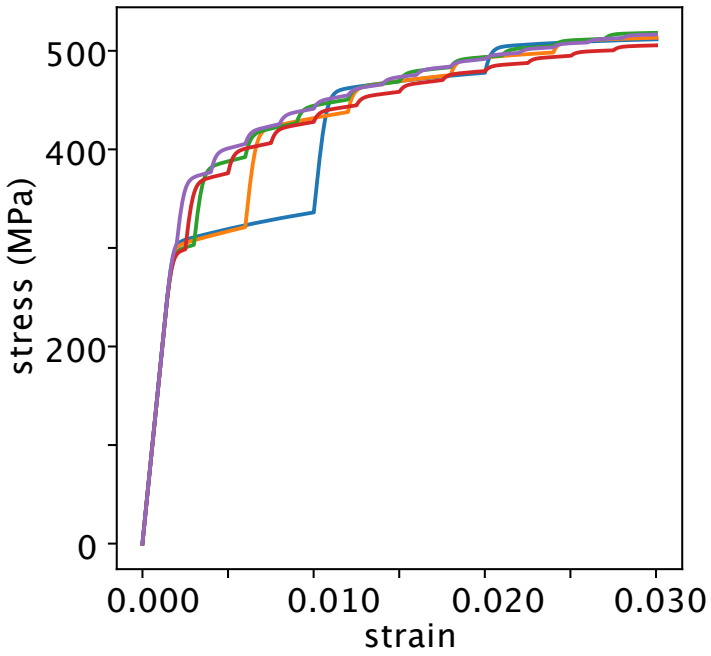

Figure 7: Synthetically generated five different strain rate jump tension tests. The five tests include 3, 5, 10, 12, and 15 strain rate jumps, and the strain rates for these jumps are corresponding linearly discretized values between strain rates of 1×10^{-5} and 1×10^{-3} s^{-1}. For example strain rate jump test with three jumps have rates 1×10^{5}, 5.05×10^{-4}, and 1×10^{-3} s^{-1}, respectively (blue curve in the plot).

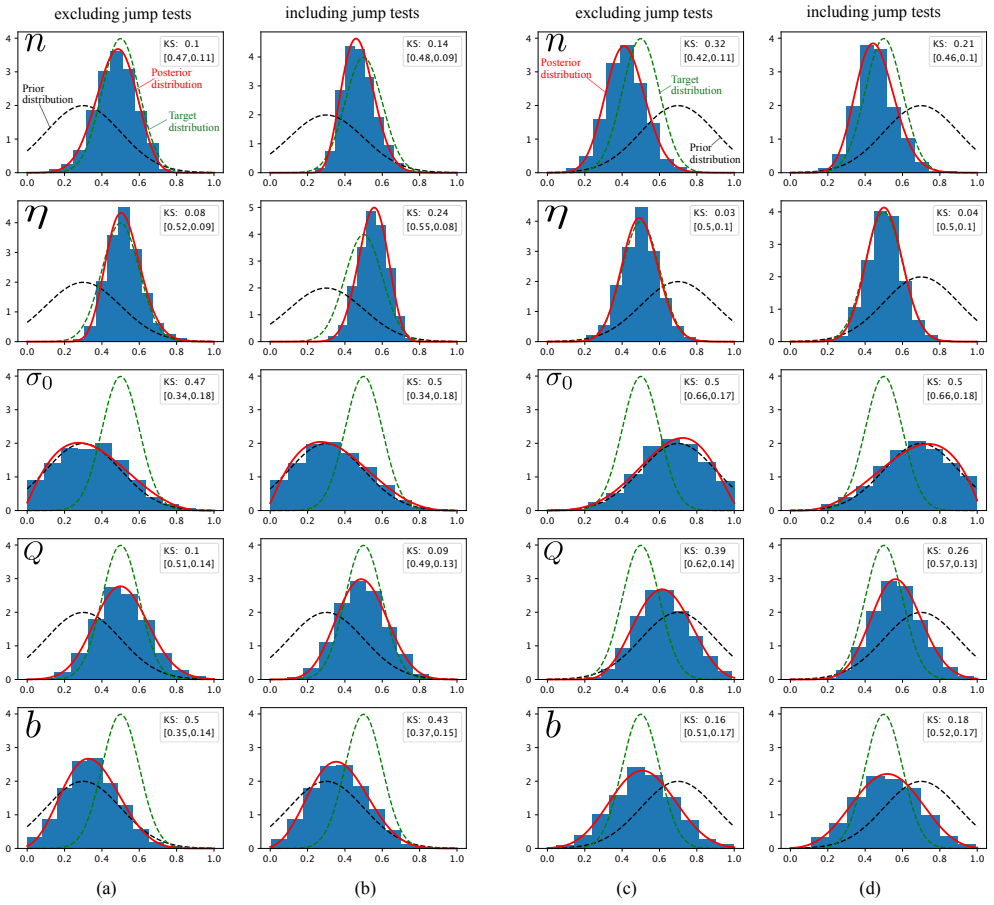

Figure 8: Posterior distributions of the five inelastic parameters obtained from tension and creep tests ((a) and (c)) and when including strain rate jump tension tests with tension and creep tests ((b) and (d)), with different truncated normal prior distributions ((a) and (b): mean 0.3 standard deviation: 0.2; (c) and (d): mean 0.7, standard deviation 0.2). The ξ in the likelihood function is fixed to unity for all the cases. Including strain rate jump tests brings the posterior distributions (red solid curves) of the sensitive parameters closer to their expected distributions (green dashed curves).

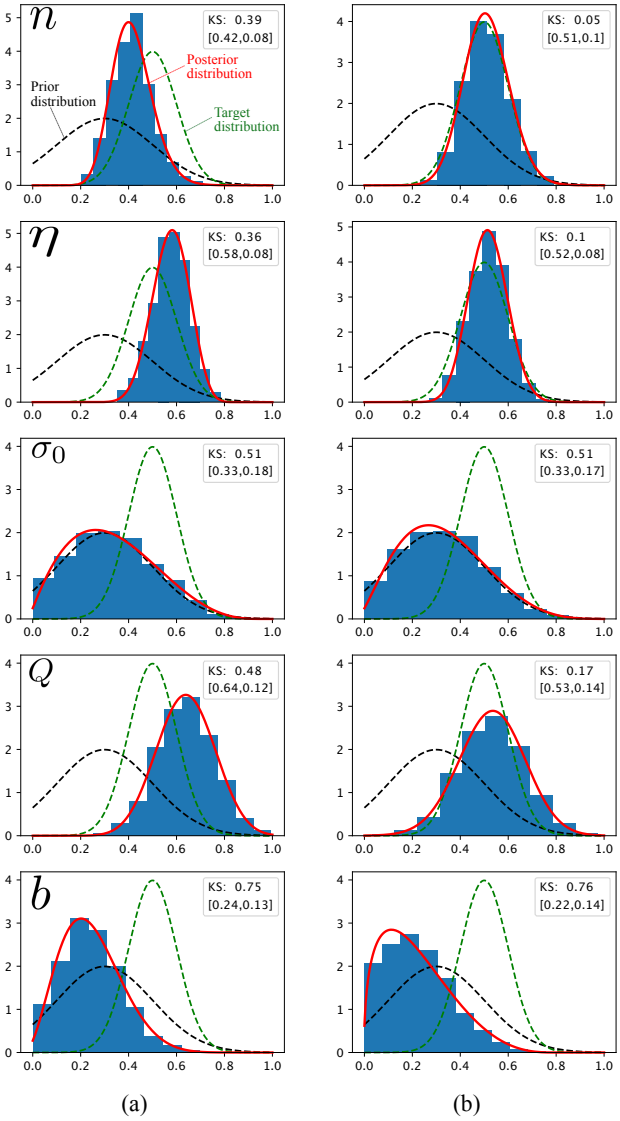

Figure 9: Posterior distributions with truncated normal priors with mean 0.3 and standard deviation of 0.2 for all the five parameters, obtained with different values of ξ in the likelihood function. Column (a) figures have $\xi = 5.0$ and 1×10^{-5} for tensile and creep tests, respectively, while for column (b) figures $\xi = 100.0$ and 1×10^{-3} for tensile and creep tests.

is fixed to unity to exclude the effect of experimental scatter on the performance of the Bayesian MCMC analysis. However, real experimental data will have some scatter associated with it, leading to a non unit value of ξ. We investigate the effect of data scatter by running the Bayesian MCMC analysis for two different values of ξ, tensile 5.0, creep 1×10^{-5}; and tensile 100.0, creep 1×10^{-3}. Figure 9 shows the resulting posterior distributions starting from truncated normal priors, mean 0.3 and standard deviation 0.2, using 10 tension and creep synthetic experiments.

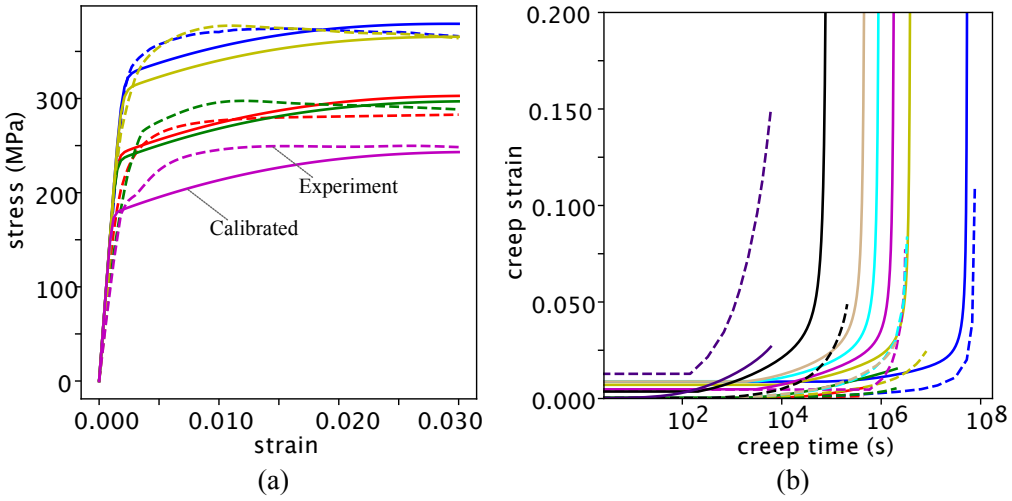

Figure 10: Calibrated mean plasticity model for Grade 91 at 600 °C for tensile (a) and creep (b) experimental conditions. The dashed lines represent experimental mean data, while the solid lines are the simulated results. Different colors represent different experimental conditions, i. e., strain rates for tensile and stresses for creep tests.

The change in the standard deviation does not significantly affect the mean of the posterior distribution for the sensitive parameters n and η. However, changing ξ does improve the standard deviation of the distributions, improving the KS comparison between the posteriors and the target distributions.

The above analysis highlights the stability of the posterior distributions from the Bayesian MCMC analysis where the synthetically generated reference data reflects accurately the underlying parameter distributions, which may not hold when using real experimental reference data.

3.2. Real experimental data

This section tests the conclusions derived from the synthetic data on a real data set of tension and creep test results for modified 9Cr-1Mo (Grade 91) steel. Grade 91 steel is a ferritic–martensitic alloy steel with good high temperature strength, making it an excellent candidate material for high temperature structural components [47]. The reference data for the likelihood function, y_i, in the Bayesian MCMC analysis consists of five tensile and ten creep tests for Grade 91 steel at 600 °C, [48–54]. The analysis considers an averaged experimental response for loading conditions duplicated by more than one experiment. The study on synthetic data demonstrates that an informed prior is required to generate an accurate posterior. To obtain the preliminary set of parameter values needed for deciding the bounds for the normal prior distributions in the Bayesian analysis we calibrate the inelastic model by minimizing the error between the experimental and simulated tensile and creep responses. Similar to the synthetic analysis, this analysis also fixes the damage parameters to those obtained from a linear Larson–Miller fit for Grade 91 steel. The dashed lines in Fig. 10 represents the experimental references used for both model calibration and Bayesian MCMC analysis. We use genetic algorithm (GA) optimization, provided in the SciPy optimize module in Python, to minimize the mean square error between the experimental and simulated tensile and creep results. The GA optimization starts with an

initial population of 15, the recombination parameter value of 0.7, and a uniform random number between 0.5 and 1.0 for the mutation parameter which are the default values in the python optimization library. Due to the high computation cost of objective function evaluation, the GA terminates when the objective function value falls below 0.02 or when the population evolutions reach 100. The optimizer minimizes the sum of the mean square error for all the tests, weighted so that the creep and tension tests contribute equally to the initial error for the initial parameter set. The optimized initial model, second column in Table 3, reasonably captures the experimental behavior for most cases (see solid lines in Fig. 10). Table 3 also lists the parameter bounds

Table 3: Calibrated inelastic parameter values to real experimental data for Grade 91 at 600 °C.

parameter	value	bounds
n	8.274	$[7, 10]$
η	747.4	$[600, 900]$
σ_0	3.550	$[2, 5]$
Q	112.0	$[80, 130]$
b	44.0	$[20, 70]$
A	650.0	
ζ	10.0	
ϕ	2.04	

used for the Bayesian MCMC analysis with the real data, which center the calibrated values. Table 4 repeats the sensitivity analysis described above for the real experimental data and a stan-

Table 4: Sensitivity values of different inelastic parameters with real experimental data.

parameter	**Sobol**	**FAST**
n	0.7116	0.6955
η	0.1341	0.1437
σ_0	0.0032	0.0044
Q	0.1330	0.1396
b	0.0485	0.0513

dard deviation, ξ, of 1.0. n and η are still the most sensitive parameters and σ_0 remains the least sensitive. The relative difference in sensitivity values of n and η with real data (≈ 0.7 and 0.14) is significantly different from those with synthetic data (≈ 0.8 for both). Thus the underlying data influences the parameter sensitivities and, in turn, the posterior distributions from the Bayesian analysis. Based on the previous results on synthetic data, the analysis for the experimental data assumes a truncated normal distribution.

Effect of prior means. Figure 11 compares the posterior parameter distributions with two different prior distribution means of 0.3 and 0.7, and with a unit ξ. The most sensitive parameter n has consistent distributions for both cases, while the results for the remaining parameters depend strongly on their prior means.

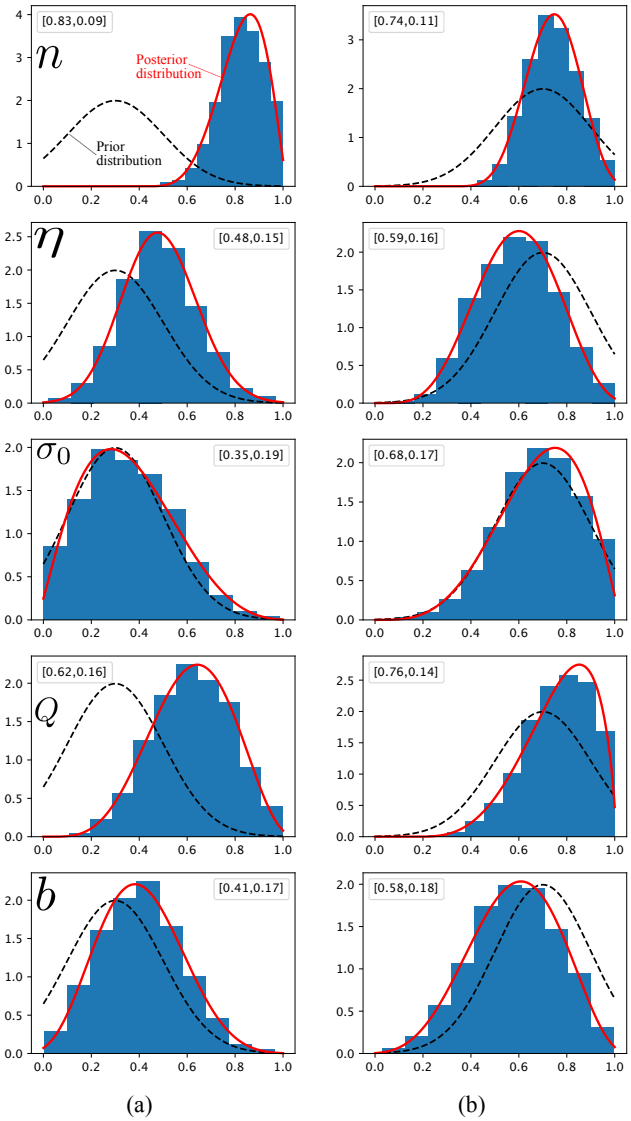

Figure 11: Posterior distributions from truncated normal priors with mean 0.3, (a), and 0.7, (b), and standard deviations of 0.2 for all the five parameters obtained with real experimental data for the Bayesian analysis. The fitted β-distributions and normalized histograms are in red and blue, respectively. The values in the top corner are the posterior mean and standard deviation.

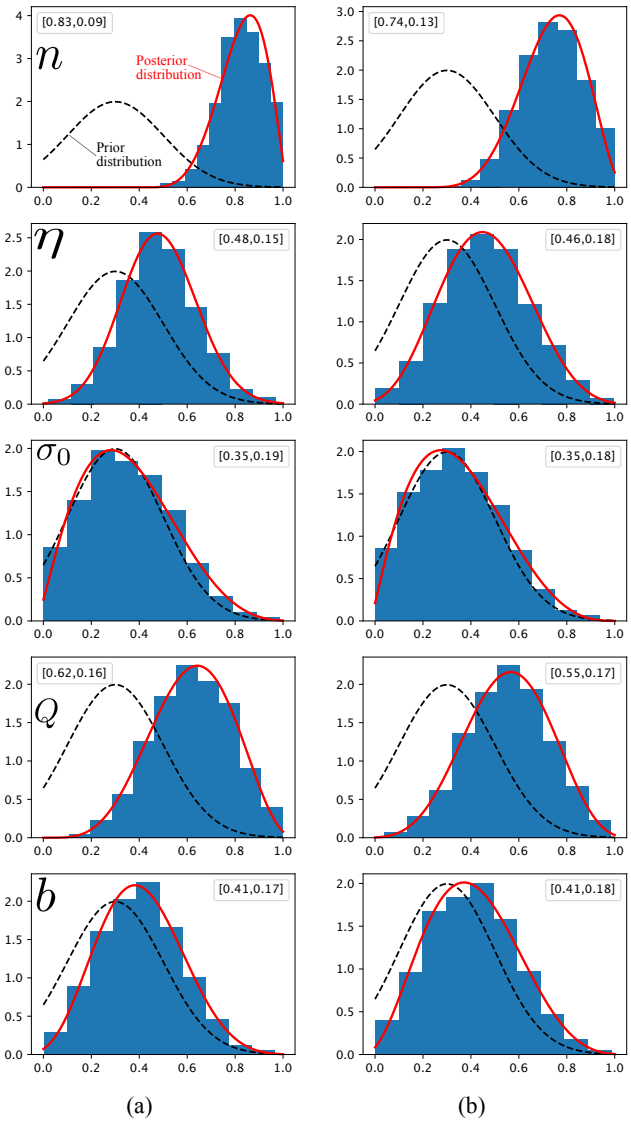

Figure 12: Posterior distributions with truncated normal priors with mean 0.3 and standard deviation of 0.2 for all the five parameters, obtained with different values of ξ in the likelihood function obtained with real experimental data for the Bayesian analysis. Column (a) figures have $\xi = 1$ for both tensile and creep tests, while for column (b) figures $\xi = 200$ and 1×10^{-3} for tensile and creep tests respectively.

Effect of data scatter. As with the synthetic data, we also investigate the effect of data scatter on the posterior distributions from the Bayesian analysis with real data by varying the ξ values in the likelihood function. Figure 12 compares the posterior distributions with unit standard deviation values for both tensile and creep likelihood functions, to that of $\xi = 200.0$ and $\xi = 1 \times 10^{-3}$ for tensile and creep cases, respectively. Similar to the result for the synthetic data, changing the

standard deviation values does not change the posterior means.[2]

4. Discussion

4.1. Sensitivity analysis

The rate sensitivity n and viscosity η are the most sensitive parameters followed by the hardening parameters Q and b, while the initial yield strength σ_0 is the least sensitive of all. Since the parameter sensitivity depends on the parameter bounds and the underlying data, we need to perform this analysis prior to running the Bayesian MCMC analysis. Quantifying the parameter sensitivity values can reduce the computation cost of the Bayesian MCMC by lowering the dimensionality of the problem (i.e., fixing the least sensitive parameters). The sensitivity information also helps to determine the reliability of the posterior distributions since less sensitive parameters are less accurately predicted.

4.2. Synthetic experimental data

This work uses synthetically generated data to test the effect of different attributes of the Bayesian analysis, decoupling spurious effects present in real experimental data. Figure 3 shows that a uniform prior distribution is unable to recover the true posterior distributions, except for the most sensitive parameters n and η. Even for the most sensitive parameters the posterior means (0.35 for n, and 0.62 for η) are different from the target values (0.5 for both n and η). The posterior mean values with the truncated normal prior (0.47 for n, and 0.52 for η) show that with an informed prior (i.e., specifying the distribution type of the data) the method can accurately recover the true solution. This is also evident from the lower Kolmogorov-Smirnov (KS) values between the posterior and target distributions with the truncated normal prior (≈ 0.1) as compared to a uniform prior distribution (more that 0.4).

Fig. 4 also demonstrates this trend where even starting with two different prior means (0.3 versus 0.7), but with the same distribution type (truncated normal), the Bayesian process recovers the true posterior distributions of the most sensitive parameters (n and η). For the less sensitive hardening parameters, when starting with a prior mean of 0.3 (Fig. 4 (a)) the resulting posterior mean of Q (0.51) is close to the target solution (0.5), while the posterior mean of hardening parameter b (0.35) is not recovered. When starting with a prior mean of 0.7 (Fig. 4 (b)) the true posterior mean for parameter b is recovered from the Bayesian analysis, but not for parameter Q. For the parameters where the true posterior means are recovered, the distribution resembles the target distribution (KS value of 0.1 for Q in Fig. 4 (a), and 0.16 for b in Fig. 4 (b)). This comparison highlights the significant effect of prior means on the posterior distributions of the hardening parameters Q and b, even though they have similar sensitivities to the likelihood.

Moreover, for the case with a prior mean of 0.3, even when increasing the amount of reference data by six times (5 versus 30 datasets Fig. 5 (a) and (b) respectively), the method still does not recover the true distribution for the hardening parameter b. This suggests increasing the amount of similar data does not increase the accuracy of the posterior distribution of the less sensitive hardening parameters. Tensile and creep test conditions are not sufficient to provide

[2]The posterior distributions obtained for all the Bayesian MCMC runs performed in this work (both with real and synthetic data) had their potential scale reduction factor values close to unity (≤ 1.07) for all parameters, indicating convergence of the five Markov chains.

complete information on the viscoplastic model parameters to the Bayesian analysis to uniquely and accurately estimate the true posterior distributions.

Reducing the dimensionality of the problem by fixing the least sensitive parameter (σ_0) does not improve the distributions of the other parameters, as demonstrated by the similar KS values for Q and b between Fig. 6 and Fig. 4 (a). In fact, the posterior distributions of the other four inelastic parameters hardly change when fixing σ_0, indicating no correlation between σ_0 with the other parameters.

Figure 8 shows that including strain rate jump tests in the reference for the Bayesian MCMC analysis improves the posterior distribution of the lesser sensitive hardening parameters (Q and b). Moreover, the improvement is consistent even when starting with different prior distributions with prior means of 0.3 ((a) and (b) in Fig. 8) and 0.7 ((c) and (c) in Fig. 8) for all the parameters. This emphasizes the importance of adding different *types* of experimental tests rather than *additional similar* experiments to enhance the performance of the Bayesian analysis.

Finally, there does not seem to be a significant difference between the posterior means with different values of standard deviation, ξ, in the likelihood function ((a): low standard deviation; (b): high standard deviation in Fig. 9). The posterior distribution of the parameters n and Q improve slightly when increasing the standard deviation, evident from lower KS values by $\approx 10\,\%$. This highlights the stability of the Bayesian approach when the underlying data successfully captures the true parameter distribution.

4.3. Real experimental data

This study also assesses the conclusions drawn from the comprehensive Bayesian MCMC analysis with synthetically generated data against real experimental data for Grade 91. The high sensitivity of the stress exponent, n, and the general trend in parameter sensitivities is consistent between the real experimental data, Grade 91 at 600 °C, and the synthetically generated data (see Tables 2 and 4). However, the relative difference in the sensitivities of n and η is much more significant in case of the real data, highlighting the influence of the underlying data on the reliability of the posterior distributions from the Bayesian analysis.

The posterior distribution for the most sensitive parameter, n, is stable to different prior means of 0.3 and 0.7 ((a) and (b) in Fig. 11), a result consistent between the real and synthetic data. For the other (less sensitive) parameters (η, Q, and b) the results are considerably dependent on the prior distributions. However, analyzing the posterior distributions from the different priors helps to identify their true solutions. For example, in case of η the shift between prior to posterior is 0.3 to 0.48 ((a) in Fig. 11) and from 0.7 to 0.59 ((b) in Fig. 11), indicating that the true solution may be somewhere close to 0.5. Similar inferences can be also drawn for the hardening parameters, Q and b. The posterior distribution of the least sensitive parameter, σ_0, hardly changes from its prior, a result also consistent between analysis with real and synthetic reference data. Hence, in order to obtain a better estimation of the true solutions of less sensitive parameters, we propose to perform multiple Bayesian runs with different prior means but having the same distribution type.

Finally, for both real experimental data and artificially generated data, varying the standard deviation value in the likelihood function, ξ, does not seem to significantly affect the posterior distribution means (Fig. 12).

5. Conclusion

This work investigates the effect of varying different aspects of the Bayesian MCMC methodology on the resulting parameter distributions for a uniaxial elasto–viscoplastic damage model using both synthetically generated and actual experimental data. The key results from the analysis with synthetic data are:

- The stress exponent n and the viscosity parameter η are the most sensitive parameters for the model, followed by the hardening parameters Q and b. σ_0 is the least sensitive of all.
- For the most sensitive parameters a uniform prior distribution recovers the target distribution type (normal) but not the correct mean.
- A normal prior distribution accurately recovers the true target distributions of the most sensitive parameters n and η, even when starting with different prior means. Thus, an informed prior distribution improves the performance of the Bayesian MCMC analysis.
- The posterior distributions do not change significantly when increasing the reference data from 5 tensile and creep test conditions to 30 tensile and creep test conditions. However, including additional strain rate jump tensile tests improves the posterior distributions of the less sensitive hardening parameters Q and b.
- Reducing the parameter dimensionality by fixing the least sensitive parameter σ_0 hardly affects the posterior distributions of the remaining parameters suggesting σ_0 is uncorrelated to the other parameters.
- Finally, the standard deviation parameter representing the effect of scatter in the experimental data, ξ in the likelihood function, has limited influence on the posterior means.

Even though the general sensitivity order of the inelastic parameters are consistent between the synthetic and the real data there appears to be a significant qualitative difference for the inelastic parameter, η. Thus, the underlying data has significant influence on the parameter sensitivities. The posterior distribution of n remains stable with different normal prior distributions with real tensile and creep data, while the other posteriors seem to be considerably influenced by the prior. Hence, to obtain a reliable statistical model a suitable method would be to perform multiple Bayesian MCMC analyses with different prior means. Analyzing the posteriors from these different priors can provide an estimate of the true solution.

This work considered a simple uniaxial, monotonic material model. Future work must repeat this analysis with an inelastic model including kinematic hardening terms to account for cyclic plasticity to produce a comprehensive statistical model of high temperature deformation and failure. Improved methods for quantifying property distributions describing material uncertainty at high temperatures will lead to safer, less costly component designs and ultimately reduce the cost and increase the available of new, efficient energy generation techniques.

Acknowledgement

AC would like to thank Arindam Fadikar and Stefan M. Wild of the Mathematics and Computer Science Division in Argonne National Laboratory for valuable discussions regarding the Bayesian approach. This work was sponsored by the US Department of Energy under Contract No. DE-AC02-06CH11357 with Argonne National Laboratory, managed and operated by

UChicago Argonne LLC. Specific programmatic support was provided by the Nuclear Energy Advanced Modeling and Simulation (NEAMS) program.

References

[1] D. Hu, R. Wang, Z. Tao, Probabilistic design for turbine disk at high temperature, Aircraft Engineering and Aerospace Technology (2011).

[2] D. Hu, Q. Ma, L. Shang, Y. Gao, R. Wang, Creep-fatigue behavior of turbine disc of superalloy gh720li at 650 c and probabilistic creep-fatigue modeling, Materials Science and Engineering: A 670 (2016) 17–25.

[3] F. Koelzow, C. Kontermann, K. Helbig, D. Jarmowski, Probabilistic lifetime assessment approach of 2%-cr steel considering material and loading profile scatter, Journal of Engineering for Gas Turbines and Power 142 (2020).

[4] R. P. Wei, D. Masser, H. Liu, D. G. Harlow, Probabilistic considerations of creep crack growth, Materials Science and Engineering: A 189 (1994) 69–76.

[5] K. Nikbin, M. Yatomi, K. Wasmer, G. Webster, Probabilistic analysis of creep crack initiation and growth in pipe components, International journal of pressure vessels and piping 80 (2003) 585–595.

[6] American Institute of Steel Construction Manual, 15 ed., 2017.

[7] J. H. Schaibly, K. E. Shuler, Study of the sensitivity of coupled reaction systems to uncertainties in rate coefficients. II Applications, Journal of Chemical Physics 59 (1973) 3879–3888. doi:doi:10.1063/1.1680572.

[8] A. F. Saleeb, A. S. Gendy, T. E. Wilt, Parameter-Estimation Algorithms for Characterizing a Class of Isotropic and Anisotropic Viscoplastic Material Models, Technical Report, 2002.

[9] R. Mahnken, M. Johansson, K. Runesson, Parameter estimation for a viscoplastic damage model using a gradient-based optimization algorithm, Engineering Computations (Swansea, Wales) 15 (1998) 925–955. doi:doi:10.1108/02644409810236920.

[10] O. T. Bruhns, D. K. Anding, On the simultaneous estimation of model parameters used in constitutive laws for inelastic material behaviour, International journal of plasticity 15 (1999) 1311–1340. doi:doi:10.1016/S0749-6419(99)00046-7.

[11] A. Andrade-Campos, S. Thuillier, P. Pilvin, F. Teixeira-Dias, On the determination of material parameters for internal variable thermoelastic-viscoplastic constitutive models, International Journal of Plasticity 23 (2007) 1349–1379. doi:doi:10.1016/j.ijplas.2006.09.002.

[12] J. C. Gelin, O. Ghouati, An inverse method for determining viscoplastic properties of aluminium alloys, Journal of Materials Processing Tech. 45 (1994) 435–440. doi:doi:10.1016/0924-0136(94)90378-6.

[13] A. F. Saleeb, T. E. Wilt, N. R. Al-Zoubi, A. S. Gendy, An anisotropic viscoelastoplastic model for composites - Sensitivity analysis and parameter estimation, Composites Part B: Engineering 34 (2003) 21–39. doi:doi:10.1016/S1359-8368(02)00078-1.

[14] A. Chakraborty, P. Eisenlohr, Evaluation of an inverse methodology for estimating constitutive parameters in face-centered cubic materials from single crystal indentations, European Journal of Mechanics, A/Solids 66 (2017) 114–124. doi:doi:10.1016/j.euromechsol.2017.06.012.

[15] J. Kajberg, B. Wikman, Viscoplastic parameter estimation by high strain-rate experiments and inverse modelling - Speckle measurements and high-speed photography, International Journal of Solids and Structures 44 (2007) 145–164. doi:doi:10.1016/j.ijsolstr.2006.04.018.

[16] T. Massé, Y. Lejeail, Creep behaviour and failure modelling of modified 9Cr1Mo steel, in: Nuclear Engineering and Design, volume 246, 2012, pp. 220–232. doi:doi:10.1016/j.nucengdes.2012.02.006.

[17] M. C. Messner, V.-T. Phan, T.-L. Sham, A Unified Inelastic Constitutive Model for the Average Engineering Response of Grade 91 Steel, ASME International, 2018. doi:doi:10.1115/pvp2018-84104.

[18] M. C. Messner, V. T. Phan, T. L. Sham, Evaluating and modeling rate sensitivity in advanced reactor structural materials: 316H, Gr. 91, and A617, International Journal of Pressure Vessels and Piping 178 (2019). doi:doi:10.1016/j.ijpvp.2019.103997.

[19] R. Sánchez-Martín, M. T. Pérez-Prado, J. Segurado, J. Bohlen, I. Gutiérrez-Urrutia, J. Llorca, J. M. Molina-Aldareguia, Measuring the critical resolved shear stresses in Mg alloys by instrumented nanoindentation, Acta Materialia 71 (2014) 283–292. doi:doi:10.1016/j.actamat.2014.03.014.

[20] T. Seibert, J. Lehn, S. Schwan, F. G. Kollmann, Identification of material parameters for inelastic constitutive models: Stochastic simulations for the analysis of deviations, Continuum Mechanics and Thermodynamics 12 (2000) 95–120. doi:doi:10.1007/s001610050130.

[21] T. Harth, S. Schwan, J. Lehn, F. G. Kollmann, Identification of material parameters for inelastic constitutive models: Statistical analysis and design of experiments, International Journal of Plasticity 20 (2004) 1403–1440. doi:doi:10.1016/j.ijplas.2003.11.001.

[22] M. C. Kennedy, A. O'Hagan, Bayesian calibration of computer models, Journal of the Royal Statistical Society: Series B (Statistical Methodology) 63 (2001) 425–464. doi:doi:10.1111/1467-9868.00294.

[23] H. Rappel, L. A. Beex, L. Noels, S. P. Bordas, Identifying elastoplastic parameters with Bayes' theorem considering output error, input error and model uncertainty, Probabilistic Engineering Mechanics 55 (2019) 28–41. doi:doi:10.1016/j.probengmech.2018.08.004.
[24] D. D. Fitzenz, A. Jalobeanu, S. H. Hickman, Integrating laboratory creep compaction data with numerical fault models: A Bayesian framework, Journal of Geophysical Research 112 (2007) B08410. doi:doi:10.1029/2006JB004792.
[25] S. Madireddy, B. Sista, K. Vemaganti, A Bayesian approach to selecting hyperelastic constitutive models of soft tissue, Computer Methods in Applied Mechanics and Engineering 291 (2015) 102–122. doi:doi:10.1016/j.cma.2015.03.012.
[26] H. Rappel, L. A. Beex, S. P. Bordas, Bayesian inference to identify parameters in viscoelasticity, Mechanics of Time-Dependent Materials 22 (2018) 221–258. doi:doi:10.1007/s11043-017-9361-0.
[27] J. Gang, J. Choi, B. Lee, J. Joo, Material parameter identification of viscoplastic model for solder alloy in electronics package using Bayesian calibration, in: Proceedings of the ASME Design Engineering Technical Conference, volume 3, 2010, pp. 827–834. doi:doi:10.1115/DETC2010-28603.
[28] J. H. Gang, D. An, J. W. Joo, J. H. Choi, Uncertainty analysis of solder alloy material parameters estimation based on model calibration method, Microelectronics Reliability 52 (2012) 1128–1137. doi:doi:10.1016/j.microrel.2012.01.008.
[29] E. Asaadi, P. S. Heyns, A computational framework for Bayesian inference in plasticity models characterisation, Computer Methods in Applied Mechanics and Engineering 321 (2017) 455–481. doi:doi:10.1016/j.cma.2017.04.017.
[30] S. R. Yeratapally, M. G. Glavicic, C. Argyrakis, M. D. Sangid, Bayesian uncertainty quantification and propagation for validation of a microstructure sensitive model for prediction of fatigue crack initiation, Reliability Engineering and System Safety 164 (2017) 110–123. doi:doi:10.1016/j.ress.2017.03.006.
[31] E. Janouchová, A. Kučerová, Bayesian inference of heterogeneous viscoplastic material parameters, Acta Polytechnica CTU Proceedings 15 (2018) 41–45. doi:doi:10.14311/app.2018.15.0041.
[32] A. Chakraborty, C. Zhang, S. Balachandran, T. R. Bieler, P. Eisenlohr, Assessment of surface and bulk-dominated methodologies to measure critical resolved shear stresses in hexagonal materials, Acta Materialia 184 (2020) 241–253. doi:doi:10.1016/j.actamat.2019.11.023.
[33] P. Perzyna, Fundamental Problems in Viscoplasticity, Advances in Applied Mechanics 9 (1966) 243–377. doi:doi:10.1016/S0065-2156(08)70009-7.
[34] J. L. Chaboche, A review of some plasticity and viscoplasticity constitutive theories, International Journal of Plasticity 24 (2008) 1642–1693. doi:doi:10.1016/j.ijplas.2008.03.009.
[35] F. A. Leckie, D. R. Hayhurst, Constitutive equations for creep rupture, Acta Metallurgica 25 (1977) 1059–1070. doi:doi:10.1016/0001-6160(77)90135-3.
[36] A. Chakraborty, M. C. Messner, T.-L. Sham, Uncertainty quantification of viscoplastic parameters for Grade 91 steel through Bayesian analysis, in: In the Proceedings of the 2020 ASME Conference on Pressure Vessels & Piping (In Press), PVP2020-21306., 2020.
[37] T. Aven, E. Zio, Some considerations on the treatment of uncertainties in risk assessment for practical decision making, in: Reliability Engineering and System Safety, volume 96, 2011, pp. 64–74. doi:doi:10.1016/j.ress.2010.06.001.
[38] R. Flage, P. Baraldi, E. Zio, T. Aven, Probability and Possibility-Based Representations of Uncertainty in Fault Tree Analysis, Risk Analysis 33 (2013) 121–133. doi:doi:10.1111/j.1539-6924.2012.01873.x.
[39] A. Der Kiureghian, O. Ditlevsen, Aleatory or epistemic? Does it matter?, Structural Safety 31 (2009) 105–112.
[40] P. E. Hadjidoukas, P. Angelikopoulos, D. Rossinelli, D. Alexeev, C. Papadimitriou, P. Koumoutsakos, Bayesian uncertainty quantification and propagation for discrete element simulations of granular materials, Computer Methods in Applied Mechanics and Engineering 282 (2014) 218–238. doi:doi:10.1016/j.cma.2014.07.017.
[41] J. Salvatier, T. V. Wiecki, C. Fonnesbeck, Probabilistic programming in Python using PyMC3, PeerJ Computer Science 2 (2016). doi:doi:10.7717/peerj-cs.55. arXiv:1507.08050.
[42] S. Chib, E. Greenberg, Understanding the metropolis-hastings algorithm, American Statistician 49 (1995) 327–335. doi:doi:10.1080/00031305.1995.10476177.
[43] C. Andrieu, N. De Freitas, A. Doucet, M. I. Jordan, An introduction to MCMC for machine learning, Machine Learning 50 (2003) 5–43. doi:doi:10.1023/A:1020281327116.
[44] I. M. Sobol, Global sensitivity indices for nonlinear mathematical models and their Monte Carlo estimates, Mathematics and Computers in Simulation 55 (2001) 271–280. doi:doi:10.1016/S0378-4754(00)00270-6.
[45] A. Saltelli, Making best use of model evaluations to compute sensitivity indices, Computer Physics Communications 145 (2002) 280–297. doi:doi:10.1016/S0010-4655(02)00280-1.
[46] J. D. Herman, W. Usher, SALib: An open-source Python library for Sensitivity Analysis., J. Open Source Software 2 (2017) 97.
[47] R. Lim, M. Sauzay, F. Dalle, I. Tournie, P. Bonnaillie, A. F. Gourgues-Lorenzon, Modelling and experimen-

tal study of the tertiary creep stage of Grade 91 steel, International Journal of Fracture 169 (2011) 213–228. doi:doi:10.1007/s10704-011-9585-y.

[48] M. Yaguchi, Y. Takahashi, Unified Inelastic Constitutive Model for Modified 9Cr-lMo Steel Incorporating Dynamic Strain Aging Effect., JSME International Journal Series A 42 (1999) 1–10. doi:doi:10.1299/jsmea.42.1.

[49] M. Yaguchi, Y. Takahashi, Ratchetting of viscoplastic material with cyclic softening, part 1: Experiments on modified 9Cr-1Mo steel, International Journal of Plasticity 21 (2005) 43–65. doi:doi:10.1016/j.ijplas.2004.02.001.

[50] B. K. Choudhary, E. Isaac Samuel, Creep behaviour of modified 9Cr-1Mo ferritic steel, Journal of Nuclear Materials 412 (2011) 82–89. doi:doi:10.1016/j.jnucmat.2011.02.024.

[51] S. Latha, M. Nandagopal, S. P. Selvi, K. Laha, M. D. Mathew, Tensile and creep behaviour of modified 9Cr-1Mo steel cladding tube for fast reactor using metallic fuel, in: Procedia Engineering, volume 86, Elsevier Ltd, 2014, pp. 71–79. doi:doi:10.1016/j.proeng.2014.11.013.

[52] K. Maruyama, J. Nakamura, K. Yoshimi, Y. Nagae, Evaluation of long-term creep rupture life of Gr. 91 steel by analysis of on-going creep curves, in: Proceedings from the Eighth International Conference on Advances in Materials Technoglogy for Fossil Power Plants, 2016, pp. 467–478.

[53] R. W. Swindeman, Cyclic stress-strain-time response of a 9Cr-1Mo-V-Nb pressure vessel steel at high temperature, in: Low Cycle Fatigue, ASTM International, 1988.

[54] K. Kimura, H. Kushima, K. Sawada, Long-term creep deformation property of modified 9Cr-1Mo steel, Materials Science and Engineering A 510-511 (2009) 58–63. doi:doi:10.1016/j.msea.2008.04.095.